IL-21 promotes myocardial ischemia/reperfusion injury through the modulation of neutrophil infiltration

Kejing Wang[1,2]*, Shuang Wen[1,2]*, Jiao Jiao[1,2]*, Tingting Tang[1,2], Xin Zhao[3], Min Zhang[1,2], Bingjie Lv[1,2], Yuzhi Lu[1,2], Xingdi Zhou[1,2], Jingyong Li[1,2], Shaofang Nie[1,2], Yuhua Liao[1,2], Qing Wang[4], Xin Tu[4], Ziad Mallat[5], Ni Xia[1,2]† and Xiang Cheng[1,2]†

[1]Department of Cardiology, Union Hospital, Tongji Medical College, Huazhong University of Science and Technology, Wuhan 430022, China;

[2]Key Laboratory of Biological Targeted Therapy of Education Ministry and Hubei Province, Union Hospital, Tongji Medical College, Huazhong University of Science and Technology, Wuhan 430022, China;

[3]Department of Cardiology, Beijing Anzhen Hospital, Capital Medical University, Beijing 100029, China;

[4]Key Laboratory of Molecular Biophysics of the Ministry of Education, Cardio-X Institute, College of Life Science and Technology and Center of Human Genome Research, Huazhong University of Science and Technology, Wuhan, China

[5]Division of Cardiovascular Medicine, Department of Medicine, University of Cambridge, Cambridge, UK, CB20 SZ

*These authors contributed equally to this article.

†Correspondence to Ni Xia, MD, PhD, and Xiang Cheng, MD, PhD, Department of Cardiology, Union Hospital, Tongji Medical College, Huazhong University of Science and Technology, Wuhan 430022, China. Phone: +86-27-85726011. E-mail: nixiaunion@163.com (to N. X.) and nathancx@hust.edu.cn (to X. C.).

BACKGROUND AND PURPOSE

The immune system plays important roles in driving the acute inflammatory response following myocardial ischemia/reperfusion injury (MIRI). Interleukin-21 (IL-21) is a pleiotropic cytokine with multiple immunomodulatory effects and its role in MIRI remains unknown.

EXPERIMENTAL APPROACH

Myocardial injury, neutrophil infiltration and expressions of neutrophil chemokines KC (CXCL1) and MIP-2 (CXCL2) were studied in a mouse model of MIRI. Effects of IL-21 on the expression of KC and MIP-2 in neonatal mouse cardiomyocytes (CMs) and cardiac fibroblasts (CFs) were determined by real-time PCR and ELISA. The signaling mechanisms underlying these effects were explored by western blotting.

KEY RESULTS

IL-21 was elevated within the acute phase of murine MIRI. Neutralization of IL-21 attenuated myocardial injury, as illustrated by reduced infarct size, decreased cardiac troponin T levels and improved cardiac function, whereas exogenous IL-21 administration exerted opposite effects. IL-21 increased the presence of cardiac-infiltrating neutrophil and increased myocardial expression of KC and MIP-2 following MIRI. Moreover, neutrophil depletion attenuated the IL-21-induced myocardial injury. Mechanistically, IL-21 was found to induce the production of KC and MIP-2 in neonatal CMs and CFs, and it enhanced neutrophil migration as revealed by a migration assay. Furthermore, we demonstrated that IL-21-mediated chemokine expression involved the activation of Akt/NF-κB signaling in CMs and p38 MAPK/NF-κB signaling in CFs.

CONCLUSIONS AND IMPLICATIONS

Our data provide novel evidence that IL-21 plays a pathogenic role in MIRI, most likely by promoting cardiac neutrophil infiltration. Therefore, targeting IL-21 may hold therapeutic potential in treating MIRI.

Key words: Interleukin-21; ischemia/reperfusion injury; inflammation; neutrophil

Abbreviations: AMI, Acute myocardial infarction; CF, cardiac fibroblast; CM, cardiomyocyte;

KC, keratinocyte-derived chemokine (CXCL1); MIP-2, macrophage inflammatory protein-2 (CXCL2); MIRI, myocardial ischemia/reperfusion injury; STAT, signal transducers and activators of transcription

Running Title: IL-21 promotes MIRI via neutrophil recruitment

Numbers of figures: 8

Introduction

Acute myocardial infarction (AMI) is one of the leading causes of death worldwide. Early reperfusion after coronary artery occlusion is the most effective strategy to protect the vulnerable myocardium and limit infarct size. However, a variety of alterations occurring at the time of blood flow restoration may paradoxically exert deleterious effects and result in additional injury, which is referred to as myocardial ischemia/reperfusion injury (MIRI). Numerous pathophysiological mechanisms are involved in MIRI, including calcium overload, dissipation of the mitochondrial membrane potential, free radical formation, endothelial dysfunction, platelet aggregation and microembolization (Turer and Hill, 2010). Furthermore, there is a growing appreciation of the role of immune activation in the pathogenesis of myocardial damage after reperfusion (Timmers *et al*., 2012; Hofmann and Frantz, 2015).

Interleukin-21 (IL-21) is a type-I cytokine produced primarily by $CD4^+$ T cell populations and natural killer (NK) T cells, as well as by $CD8^+$ T cells and gamma delta (γδ) T cells (Sutton *et al*.,2009; Spolski and Leonard, 2014). IL-21 exerts broad immunomodulatory effects and is implicated in antitumor and antiviral responses, as well as in inflammatory responses, where it promotes the development of autoimmune diseases and certain inflammatory disorders (Parrish-Novak *et al*., 2000; Spolski and Leonard, 2008). IL-21 signals through a heterodimeric receptor complex formed by its unique receptor IL-21R and the common cytokine receptor gamma chain, γ_c. IL-21R is widely expressed by immune cells, including T cells, B cells, NK cells, NKT cells, dendritic cells, macrophages and neutrophils (Spolski *et al*., 2014). More recently, the expression of IL-21R was also described in non-immune cells, such as epithelial cells (Caruso *et al*., 2007a; Caruso *et al*., 2007b), fibroblasts (Jungel *et al*., 2004; Monteleone *et al*., 2006), keratinocytes (Caruso *et al*., 2009; Distler *et al*., 2005), endothelial cells (Wang *et al*., 2015), and neurons (Clarkson *et al*., 2014; Tzartos *et al*., 2011), suggesting the possibility that IL-21 may modulate additional inflammatory pathways besides its regulatory effects on humoral and cellular immunity. Recent findings suggest an early elevation of IL-21 following liver IRI in mice, which may be partially responsible for NK cell-mediated liver injury (Feng *et al*., 2012). Clarkson *et al*. reported that in a mouse model of transient focal brain ischemia, IL-21 was highly up-regulated in ischemic brain tissues and played a pathogenic role (Clarkson *et al*., 2014).

However, potential implications of IL-21 in relation to MIRI are still far from complete.

In this study, we demonstrated that IL-21 was elevated during the acute phase following MIRI. CD4+ T cells were a major source of IL-21 production. Neutralization of endogenous IL-21 protected against myocardial injury, whereas exogenous IL-21 administration aggravated myocardial injury. IL-21 increased the infiltration of neutrophil following MIRI and increased myocardial expression of CXC chemokines keratinocyte-derived chemokine (KC) and macrophage inflammatory protein-2 (MIP-2). Depletion of neutrophil abrogated the IL-21-induced myocardial injury. Furthermore, IL-21 directly increased the expression of KC and MIP-2 in cardiomyocytes (CMs) and cardiac fibroblasts (CFs) *in vitro*. The potential signaling mechanisms underlying these responses may involve the Akt, p38 MAPK, and NF-κB signaling pathways.

Methods

Animal model and treatments

Animal studies are reported in accordance with the ARRIVE guidelines (Kilkenny *et al*., 2010; McGrath and Lilley, 2015). Male C57BL/6 mice aged 8-12 weeks (weight 20-24g) were purchased from Wuhan University (Wuhan, China), and maintained on a chow diet in a 12-hour light/12-hour dark environment at 25 °C in the Tongji Medical School Animal Care Facility. The treatment and care of studied animals were approved by the Animal Care and Utilization Committee of Huazhong University of Science and Technology. The experimental procedures used in the work were as humane as possible. A murine MIRI model was established by temporary occlusion of the left anterior descending (LAD) coronary artery as previously described (Bohl *et al*., 2009; Michael *et al*., 1995; Tarnavski *et al*., 2004). Briefly, mice were anesthetized by intraperitoneal injection of ketamine (50 $mg \cdot kg^{-1}$) and pentobarbital sodium (50 $mg \cdot kg^{-1}$) and ventilated through a rodent respirator. The adequacy of anesthesia was assessed by testing corneal reflexes and motor responses to tail pinch. Hearts were exposed by left thoracotomy and LAD was visualized and ligated using 6-0 suture around fine PE-10 tubing with a slip knot. Sham-operated animals were subjected to the same surgical procedures without LAD ligation.

For the measurement of IL-21/IL-21R expression patterns, C57BL/6 mice were randomly subjected to a sham procedure or to 30 minutes of ischemia followed by 30 min or 1, 6, 12, or 24 hours of reperfusion (n=6 per group). To elucidate the causative role of IL-21 in this process, mice were randomly assigned to four groups. In the (1) anti-IL-21 treatment group (anti-IL-21, n=9) and the (2) isotype control antibody treatment group (isotype, n=9), mice were i.v. with 0.2 ml PBS, 100 μg of anti-IL-21 neutralizing mAb or an isotype control mAb 5 min prior to reperfusion. In the (3) recombinant mouse-IL-21 treatment group (IL-21, n=10) and the (4) vehicle treatment group (vehicle, n=11), mice were i.v. with 0.2 ml PBS containing 0.5% bovine serum albumin or 1 μg of recombinant mouse IL-21 diluted in 0.2 ml PBS containing 0.5% bovine serum albumin 5 min prior to reperfusion. For the neutrophil depletion study, the mice were randomly divided into five groups: (1) the PBS treatment group (n=5), (2) the isotype control mAb treatment group (n=5), (3) the anti-Ly6G mAb treatment group (n=5), (4) the isotype control mAb with IL-21 treatment group (n=5), and (5) the anti-Ly6G mAb with IL-21 treatment group (n=5). 250 μg of isotype control mAb or anti-Ly6G mAb dissolved in 0.2 ml PBS was i.p. one day before surgery. 1 μg of recombinant mouse IL-21 was injected intravenously 5 min prior to reperfusion.

Echocardiographic analysis of cardiac function

At the end of a 1-day reperfusion period, mice were anesthetized with inhaled 2% isoflurane/oxygen mixture and two-dimensional echocardiographic views of the mid-ventricular short axis and the parasternal long axes were obtained using a Vevo 2100 high-resolution microimaging system (VisualSonics, Toronto, Ontario, Canada) by a technician who was blinded to treatment groups. Left ventricular ejection fraction (EF) and fractional shortening (FS) were calculated from the digital images using a standard formula as previously described (Li *et al.*, 2007) .

Serum troponin T

Blood concentrations of troponin T (cTnT) were measured as an index of cardiac cellular damage using a quantitative rapid assay kit (Roche Diagnostics GmbH, Mannheim, Germany) as previously described (Metzler *et al.*, 2001).

Measurement of area at risk and infarct size

Infarct size after MIRI was determined as previously described (Bohl *et al*., 2009; Michael *et al*., 1995). Briefly, after 24 h of reperfusion, mice were anesthetized and the LAD was re-occluded at the previous ligation. 1% Evans blue was injected, and the heart was quickly excised, frozen, and cut into transverse sections below the ligature. These sections were then incubated with 1% 2,3,5-triphenyltetrazolium chloride (TTC) solution. Left ventricular area (LV), area at risk (AAR) and infarct area (I) were analyzed as described (Bohl et al., 2009) using Image-Pro Plus 6.0 software. The measurement was carried out by an investigator who was blinded to the experimental groups.

Heart-infiltrating cell isolation and flow cytometry analysis

Heart-infiltrating leukocytes were isolated as previously described, with some modifications (Liao *et al*., 2012). Briefly, following euthanasia by cervical dislocation, ischemic tissue was excised and single-cell suspensions were obtained via the digestion of ischemic myocardium with 0.1% collagenase B solution. Thereafter, granulocytes were enriched through density gradient centrifugation using Ficoll (Histopaque-1119). For the analysis of neutrophil infiltration in ischemic tissue, the cells were labeled with PE-cy7 anti-mouse CD11b and PE anti-mouse Ly-6G/Gr-1. For the analysis of IL-21-secreting leucocytes, the cells were labeled with FITC anti-mouse CD45, PE anti-mouse IL-21, Percp-cy5.5 anti-mouse CD3, PE-cy7 anti-mouse CD4 and APC anti-mouse γδTCR. Stained cells were measured via FACS Calibur flow cytometry (BD Biosciences, San Jose, CA, USA), and data were analyzed using CellQuest software (BD Biosciences) by a technician who was blinded to treatment groups. Caltag Counting Beads (Invitrogen Life Technologies, USA) were used to calculate the absolute number of cells.

Cell isolation and culture

Neonatal cardiomyocytes (CMs) were isolated from ventricles of 1-day-old C57BL/6 mice using previously described methods with some modifications (Rui *et al*., 2001). Briefly, neonatal mice were euthanized by cervical dislocation and their ventricles were minced and digested with Liberase TH (0.1 $U \cdot mL^{-1}$ in Hanks' balanced salt solution (HBSS)). After being filtered through a nylon cell strainer (70 μm size, BD Falcon, Franklin Lakes, NJ), the collected cells were incubated in 5% CO_2 at 37°C for 1 hour. Cardiac fibroblasts (CFs) were separated from CMs via differential plating, during which CMs did not attach to the culture flasks. The cells were then separately cultured with high-glucose DMEM cell culture containing 10% fetal bovine serum,

1% penicillin and streptomycin. CMs were used in experiments after they had formed a confluent monolayer and were contracting in synchrony at 72 hours. CFs from passages 2 and 3 were used for the experiment.

Neutrophils were isolated from the marrow of the femurs and tibias of adult mice through density gradient centrifugation as previously described (Lowell *et al*., 1996; Siemsen *et al*., 2007). Briefly, following euthanasia by cervical dislocation, the long bones of the hind legs were removed, and the ends were clipped. The bone marrow cells were flushed from the tibias and femurs with HBSS and filtered through a cell strainer (40 μm size, BD Falcon). The suspension was subject to a Percoll (GE Healthcare, Sweden) step gradient. Cells were collected from the neutrophil-enriched fraction, followed by a further isolation with Histopaque 1119. Purity of neutrophils was evaluated by flow cytometry (Ly-6G/Gr-1 and CD11b double-positive cells >85%).

ELISA

Levels of KC and MIP-2 in the conditioned supernatant were quantified using commercial ELISA kits (R&D Systems, Minneapolis, MN, USA) according to the manufacturer's instructions. The absorbance of each well was determined at 450 nm using a microplate reader (Elx800, Bio-Tek, USA).

Neutrophil migration assays

Neutrophil migration was measured using transwell inserts with polycarbonate filter (5-μm pores, Corning, New York, USA) preloaded in 24-well tissue culture plates. Freshly isolated neutrophils (1×10^6 cells) were added to the upper chambers of the transwell inserts, and conditioned supernatants from CMs or CFs were added to the lower well. After 60 min of incubation, the number of migrated neutrophils in the lower chamber was counted in five randomly chosen fields using an inverted microscope (Ruddy *et al*., 2004). The analysis was carried out by an investigator who was blinded to the experimental groups.

Quantitative RT-PCR (qRT-PCR)

Total RNA was extracted from ischemic tissue or cells using Trizol (Invitrogen, Carlsbad, CA, USA) and reverse transcribed into cDNA using the PrimeScript RT reagent kit (Takara Biotechnology, Dalian, China) according to the manufacturer's instructions. The mRNA levels of

the target genes were quantified using SYBR Green Master Mix (Takara Biotechnology, Dalian, China) with the CFX96 Real-Time PCR Detection System (Bio-Rad, Berkeley, CA, USA). Data from each sample were normalized to β-actin. The primer sequences are shown in Supporting Information Table S1.

Western blotting

Protein extracted from tissues or cells was separated on 10-12% sodium dodecyl sulfate (SDS)-polyacrylamide electrophoresis gels and transferred to polyvinylidene difluoride membranes. After being blocked with 5% skimmed milk in Tris-buffered saline (TBS)(1×) for 2 hours, the membranes were incubated with indicated primary antibodies at 4°C overnight, followed by incubation with HRP-conjugated secondary antibody for 2 hours. The specific bands were detected using the Super ECL reagent (Pierce, Rockford, IL). Images were obtained and analyzed using Image Lab 3.0 software. The intensity of the GAPDH band was used as a loading control for comparison between samples.

Statistical analysis

The data and statistical analysis in the present study comply with the recommendations on experimental design and analysis in pharmacology (Curtis *et al*., 2015). Data were collected and analyzed in a blinded manner. Data are presented as the means ± SEM. For normally distributed data, differences were evaluated using unpaired Student's t test between two groups. When comparing ≥3 different groups, One-way ANOVA followed by Tukey post hoc test was used for multiple comparisons, and Dunnett post hoc test was used when comparing each group with a control, only if F reached significance and there was no significant variance inhomogeneity. All analyses were performed using SPSS 13.0 (SPSS, Chicago, IL), and statistical significance was set at $P < 0.05$ (two-tailed).

Materials

Anti-mouse IL-21 monoclonal antibody (clone: FFA21), isotype control antibody (clone: eBR2a), PE-cy7 anti-mouse CD11b, PE anti-mouse Ly-6G/Gr-1, FITC anti-mouse CD45, PE anti-mouse IL-21, Percp-cy5.5 anti-mouse CD3, PE-cy7 anti-mouse CD4 and APC anti-mouse γδTCR were

obtained from eBioscience (San Diego, CA, USA). Recombinant mouse-IL-21 and primary antibodies to mouse IL-21 and IL-21R were purchased from R&D Systems (Minneapolis, MN, USA). Anti-mouse anti-Ly6G monoclonal antibody (clone: 1A8) and isotype control antibody (clone: RTK2758) were obtained from Biolegend (San Diego, CA, USA). Recombinant murine TNF-α was purchased from PeproTech Inc. (Rocky Hill, NJ, USA). Evans blue, 2,3,5-triphenyltetrazolium chloride (TTC), hydrogen peroxide (H_2O_2) solution, bovine serum albumin and Histopaque-1119 were purchased from Sigma-Aldrich (St. Louis, MO, USA). LY294002 and antibodies to phospho-Akt (Ser473), phospho-p38 (Thr180/Tyr182), phospho-ERK (Thr202/Tyr204), phospho-NF-kappa-B p65 (Ser536), phospho-Stat1 (Tyr701), phospho-Stat3 (Tyr705), Akt, p38 MAPK, ERK, NF-kappa-B p65, Stat1 and Stat3 were purchased from Cell Signaling Technology (Danvers, MA, USA). Antibody against GAPDH was purchased from AntGene (Wuhan,China). BAY11-7082 and SB203580 were obtained from Selleckchem (Houston, TX, USA). Collagenase B and Liberase TH was obtained from Roche Diagnostics GmbH (Mannheim, Germany). High-glucose DMEM, Hanks' balanced salt solution (HBSS) and fetal bovine serum were purchased from GIBCO (Carlsbad, CA, USA).

Results

Increased expression of IL-21 and its receptor in the myocardium post-reperfusion

We first examined the expression kinetics of IL-21 in the ischemic myocardium via quantitative real-time PCR. As illustrated in Figure 1A, mRNA expression of IL-21 increased rapidly within 30 min after reperfusion, peaked at 6 h and remained elevated but with a declining trend for up to 24 h. Likewise, protein expression of IL-21 was up-regulated as early as 30 min after reperfusion, reaching peak expression at 24 h (Figure 1B). Multiple cell types, including T cells, and innate immune cells, could produce IL-21 (Clarkson *et al*., 2014; Sutton *et al*., 2009). To determine which leucocytes account for the increase of IL-21 in the ischemic myocardium，we used intracellular cytokine staining combined with staining for some surface markers. Over 80% of the IL-21-secreting leukocytes were $CD3^+$ T cells, including about 77% $CD4^+$ cells and 1% $\gamma\delta TCR^+$ cells, indicating that $CD4^+$ cells were the major source of IL-21 (Figure 1E).

IL-21 exerts biological effects through binding to its receptor, a heterodimer of IL-21R and the common cytokine receptor γ_c. In the present study, we found that both mRNA and protein

expression levels of IL-21R were increased at 12 h (2.5±0.6-fold and 1.7±0.2-fold, respectively) and that they remained elevated until 24 h (4.0±0.4 and 1.8±0.2-fold, respectively) (Figure 1C and D). Furthermore, in our vitro study, we found that IL-21R gene expression in neonatal mouse CMs was increased at 1 h and reached a peak at 8 h after the induction of oxidative stress with H_2O_2. Meanwhile, the mRNA expression of IL-21R in CFs was increased at 4 h and reached a peak at 12 h after treated by TNF-α (Supporting Information Figure S1).

Neutralization of endogenous IL-21 attenuates myocardial injury, whereas exogenous IL-21 aggravates it

The early up-regulation of IL-21 and its specific receptor IL-21R in post-ischemic myocardium indicates a potential role of IL-21 in MIRI. Therefore, we examined the functional significance of IL-21 on MIRI by treating mice with an anti-IL-21 neutralizing antibody or recombinant IL-21 before reperfusion. In comparison to the effects observed in isotype-treated mice, anti-IL-21 neutralizing antibody administration reduced infarct size decreased cTnT levels and restored cardiac function as shown by improved left ventricular ejection fraction (EF) and fractional shortening (FS). In contrast, exogenous IL-21 administration significantly increased infarct size, elevated cTnT levels, and reduced cardiac function in comparison to the effects observed in vehicle-treated mice. Collectively, these findings indicated that IL-21 played a pathogenic role in MIRI (Figure 2).

IL-21 mediates neutrophil recruitment through the regulation of CXC chemokines in vivo

Infiltrated inflammatory cells play key roles in the extension of myocardial ischemic injury. Of these cells, neutrophils are the predominant type that accumulates in the reperfused myocardium within the first hours after reperfusion (Yan *et al*., 2013; Dreyer *et al*., 1991). To determine whether IL-21 is involved in neutrophil recruitment in the context of MIRI, we analyzed the absolute counts and frequency of $CD11b^{+}Gr\text{-}1^{+}$ neutrophils infiltrating the ischemic myocardium 3 h after reperfusion via flow cytometry. In comparison to infiltration in sham-operated mice, there was an obvious increase in neutrophil infiltration in the reperfused myocardium (I/R-mice). Moreover, exogenous IL-21 administration further increased neutrophil infiltration (Figure 3A-3B), while anti-IL-21 neutralizing antibody treatment reduced neutrophil infiltration (Figure 3C-3D). To examine whether neutrophils are directly related to the myocardial ischemic injury

after exogenous IL-21 administration, we conducted a neutrophil depletion study. After depletion of neutrophils by anti-Ly6G antibody, the number of neutrophils infiltrating the ischemic myocardium was markedly declined (Supporting Information Figure S2A). Furthermore, depletion of neutrophils in mice treated with exogenous IL-21 decreased infarct size, declined cTnT levels and improved cardiac function compared with isotype antibody group (Supporting Information Figure S2B-D). These results indicated that neutrophils were essential for IL-21-induced myocardial ischemic injury.

ELR-containing CXC chemokines KC, MIP-2 and lipopolysaccharide-induced CXC chemokine (LIX) are reported to be potent neutrophil chemoattractants (Frangogiannis and Entman, 2005). Therefore, we further investigated the potential effects of IL-21 on the myocardial expression of these chemokines via real-time PCR. Relative to the effects in vehicle-treated mice, IL-21 administration rapidly up-regulated KC and MIP-2 mRNA expression as early as 30 min after reperfusion. This elevation persisted for 3 h for MIP-2. However, no significant changes were observed in the expression of LIX (Figure 3E). In addition, the mRNA expression of KC and MIP-2 was reduced in the ischemic myocardium after neutralization of endogenous IL-21 (Figure 3F).

IL-21 promotes neutrophil migration and the expression of KC and MIP-2 in CMs and CFs

To determine the direct effects of IL-21 on different cell types involved in this process, we isolated neutrophils from adult mouse bone marrow and prepared CM/CF primary cultures from neonatal mice. Neutrophil migration assays indicated an enhanced neutrophil migration in the presence of conditioned medium from CMs or CFs treated with IL-21, relative to the effects observed in the presence of conditioned medium from unstimulated cells (Figure 4A). We then examined the effects of IL-21 on the expression of KC/MIP-2 in CMs and CFs. As shown in Figure 4B, IL-21 up-regulated KC and MIP-2 mRNA expression in CMs and CFs. Moreover, as detected via ELISA, IL-21 also increased KC and MIP-2 secretion by both CMs and CFs (Figure 4C).

Signaling mechanisms underlying the effects of IL-21

IL-21-mediated cellular effects have been reported to be associated with the ERK, p38 MAPK,

PI3K/Akt, NF-κB and STAT1/3 signaling pathways (Pelletier *et al*., 2004; Caruso *et al*., 2007a,b; de Totero *et al*., 2008; Xing *et al*., 2016), which are also involved in MIRI (Lopez-Neblina and Toledo-Pereyra, 2006). To further elucidate the mechanisms by which IL-21 affects MIRI, we focused on these signaling pathways. We first explored the time-course changes of these signaling pathways in the myocardium. We found that reperfusion increased the phosphorylation of ERK, p38 MAPK and NF-κB p65 as early as 10 min, while the activation of Akt, STAT1 and STAT3 occurred at 30 min after reperfusion (Supporting Information Figure S3). We further examined the effects of IL-21 on each signaling pathway at both 10 and 30 min after reperfusion. As shown in Figure 5, IL-21 further increased the phosphorylation of p38 MAPK at both 10 and 30 min after reperfusion and enhanced NF-κB p65 activation at 30 min after reperfusion.

To examine the direct effects of IL-21 on isolated CMs/CFs, we assessed the activation kinetics of the above-mentioned signaling pathways at a cellular level. As demonstrated in Figure 6, CMs and CFs responded to IL-21 with different signaling kinetics, suggesting a cell-type-specific response. In CMs, the phosphorylation of Akt was enhanced by IL-21 administration at early time points (10-30 min), and it then returned to baseline at 1 h. NF-κB p65 phosphorylation was induced within 30 min of IL-21 administration and remained elevated for up to 2 h. Stimulation with IL-21 in CFs induced the activation of p38 MAPK signaling within 30 min, which remained elevated for 2 h. NF-κB p65 phosphorylation was induced at 1 h and was maintained for up to 2 h. However, the activity of Akt in IL-21-treated CFs presented an opposite trend in comparison to that observed in CMs, showing a slightly inhibited activity at 30-60 min after IL-21 administration. There were no significant changes in the activity of the ERK, STAT1 or STAT3 signaling pathways following stimulation with IL-21 in either CMs or CFs (data not shown).

IL-21 induces KC and MIP-2 expression through Akt/NF-κB or p38 MAPK/ NF-κB signaling

Next, we examined whether the IL-21-dependent up-regulation of CXC chemokines is associated with IL-21-mediated activation of Akt, p38 MAPK and NF-κB signaling. CMs were pre-incubated with Akt inhibitor (LY294002 10 μM) or NF-κB inhibitor (BAY11-7082 10 μM), while CFs were pre-incubated with p38 MAPK inhibitor (SB203580 10 μM) or BAY11-7082. IL-21 was then added to the culture media, and the mRNA and protein expressions of KC and

MIP-2 were assessed via real-time PCR and ELISA. The short-term incubation of the inhibitors had no effect on the basal levels of chemokine expressions in both CMs and CFs. Pre-incubation with either the Akt or NF-κB inhibitor abolished the IL-21-induced KC and MIP-2 mRNA expression in CMs, whereas KC and MIP-2 secretions in the presence of IL-21 were partially inhibited by either LY294002 or BAY11-7082 (Figure 7A and B). In CFs, the inhibition of either p38 MAPK or NF-κB significantly reduced the IL-21-mediated up-regulation of KC and MIP-2 mRNA expression. Likewise, the IL-21-induced KC and MIP-2 secretions were partially inhibited by either SB203580 or BAY11-7082 (Figure 7C and D).

Our previous time-course study indicated that the IL-21-induced phosphorylation of Akt and p38 MAPK preceded the phosphorylation of NF-κB in CMs and CFs, respectively. Therefore, we further assessed whether Akt or p38 MAPK act as upstream regulators. We found that a pre-incubation with Akt or p38 MAPK inhibitors partially reduced IL-21-induced activation of NF-κB signaling in CMs or CFs, respectively, suggesting that NF-κB activation may occur, at least in part, downstream of Akt and p38 MAPK signaling following IL-21 exposure (Figure 7E and F).

Discussion and conclusions

The current study demonstrates a key role for IL-21 in myocardial injury in MIRI mice models. The data revealed that IL-21 was elevated during the acute phase of MIRI, and $CD4^+$T may be a major source of IL-21 production. Treatment with exogenous IL-21 markedly exacerbated the myocardial injury, which was related to an increase in KC and MIP-2 expression and infiltration of neutrophils. Treatment with anti-IL-21 mAb induced the opposite effect. In vitro studies revealed that IL-21 could induce KC and MIP-2 expression, mainly through Akt/NF-κB signaling in CMs and p38 MAPK/NF-κB signaling in CFs. Furthermore, the neutrophil depletion study confirmed that IL-21 aggravated myocardial injury mainly via increased neutrophil infiltration.

Emerging evidence has suggested that IL-21 mediates multiple types of tissue damage, and is an exacerbating factor in the pathogenesis of several inflammatory diseases, including inflammatory bowel disease, experimental autoimmune encephalomyelitis, rheumatoid arthritis, psoriasis, and type I diabetes (Di Fusco *et al*., 2014; Gharibi *et al*., 2016; Monteleone *et al*.,

2009). Moreover, IL-21 has also been explored as a biomarker associated with the development of coronary artery disease (Ding *et al*., 2014) and left ventricular remodeling after acute myocardial infarction (Weir *et al*., 2012). However, the pathological role of IL-21 in the acute inflammatory response, especially during ischemia/reperfusion injury, remains largely unknown.

In a mouse model of MIRI, we observed an early up-regulation of IL-21 and its functional receptor in the myocardium, supporting the hypothesis that IL-21 acts in the early stage of MIRI. Several immune cells have been reported to produce IL-21, including $CD4^+$T cells, γδT cells, neutrophils and NKT cells (Coquet *et al*., 2007; Sutton *et al*., 2009; Puga *et al*., 2012; Clarkson *et al*., 2014).. Our study revealed that $CD4^+$T cells mainly account for the production of IL-21 during MIRI. We further demonstrated that neutralization of endogenous IL-21 attenuated myocardial injury; conversely, exogenous IL-21 administration increased infarct size and reduced cardiac function. This observation is consistent with prior studies showing that IL-21 plays a pathogenic role in tissue I/R injury. Feng *et al*. have reported an increase of IL-21 production at the initial stage of mouse liver IRI, which led to IL-17A production by NK cells, and promoted liver injury (Feng *et al*., 2012). More recently, IL-21 was found to be robustly up-regulated in mice within 24 h after cerebral reperfusion injury and to contribute to both immediate and delayed brain injury (Clarkson *et al*., 2014).

Neutrophils are the most abundant leukocytes subset present during the first hours after ischemia reperfusion in the myocardium (Yan *et al*., 2013; Dreyer *et al*., 1991), and their infiltration is considered to be a critical event in MIRI, serving as the major source of reactive oxygen species and proteolytic enzymes (Vinten-Johansen, 2004). Previous evidence suggested that IL-21 may be involved in neutrophil recruitment and activation. IL-21 has been shown to indirectly induce the accumulation of neutrophils in a murine air-pouch model (Pelletier *et al*., 2004) and enhance lung infiltration by neutrophils through up-regulation of KC expression (Spolski *et al*., 2012). Recent research by Takeda *et al*. indicates that IL-21 up-regulates the surface expression of CD11b and CD16 and enhances the phagocytic ability and ROS production of human peripheral blood neutrophils (Takeda *et al*., 2014). Despite the above-mentioned findings, whether IL-21 affects neutrophil recruitment in relation to tissue ischemic reperfusion injury had not yet been examined. Our *in vivo* study shows that IL-21 can induce myocardial neutrophil infiltration during the early stage of reperfusion through the induction of KC and

MIP-2 expression. Whereas, neutralization of endogenous IL-21 reduced the number of neutrophil infiltration and expression of KC and MIP-2 in myocardial tissue. Our *in vitro* study further confirmed that IL-21 has direct effects on CMs and CFs, inducing KC and MIP-2 expression at both the mRNA and protein levels, and enhancing the migratory ability of neutrophils.

In subsequent experiments, we investigated the signaling mechanisms underlying the IL-21-mediated effects. IL-21 has been previously reported to activate several signaling pathways, including JAK-STAT (primarily STAT1 and STAT3), ERK, p38 MAPK, PI3K/Akt, and NF-κB in different tissues and cell types (Brenne *et al*., 2002; Caruso *et al*., 2009; Caruso *et al*., 2007; Caruso *et al*., 2007; Pelletier *et al*., 2004; Wang *et al*., 2015; Xing *et al*., 2016). Moreover, these signaling pathways are also known to be involved in the processes associated with MIRI (Lopez-Neblina *et al*., 2006). Our *in vivo* study indicated that IL-21 activates p38 MAPK and NF-κB signaling, which are both important in the production of various pro-inflammatory mediators, including cytokines, chemokines and adhesion molecules (Van der Heiden *et al*., 2010). At a cellular level, IL-21 induced Akt and, subsequently, NF-κB p65 activation in CMs, while in CFs, IL-21 induced the phosphorylation of p38 MAPK, which preceded the activation of NF-κB p65. Because Akt signaling was slightly inhibited in CFs after IL-21 stimulation, the opposite effects of IL-21 on CMs and CFs may explain why the activation of Akt was not observed in the ischemic myocardium *in vivo*.

NF-ϰB has been characterized as a critical transcriptional factor that regulates most chemokines at the level of transcription, and several signaling pathways are reported to regulate the upstream of NF-ϰB, including p38MAPK and PI3K/Akt. Previous reports indicated that up-regulation of CXC chemokines could be induced by NF-ϰB activation via the PI3K/Akt/IKK pathway in various cell types (Lee *et al*., 2012; Li *et al*., 2003; Li *et al*., 2015; Lin *et al*., 2011). In the present study, the involvement of Akt/NF-κB or p38 MAPK/NF-κB signaling in IL-21-mediated chemokine expression was further confirmed by using relevant signaling inhibitors, and the results of this inhibition were consistent with previous evidence indicating that CXC chemokine expression is induced via the activation of p38 MAPK, PI3K/Akt and NF-κB signaling in different cellular contexts (Lafontant *et al*., 2006; Stephanou, 2002; Turner *et al*., 2011). However, it should be noted that although the inhibition of Akt and NF-κB signaling

could substantially suppress IL-21-induced KC/MIP-2 mRNA expression, it only reduced but did not abrogate IL-21-induced secretion of KC/MIP-2 in CMs. Likewise, the inhibition of p38 MAPK and NF-κB signaling also partially inhibited the IL-21-induced secretion of KC/MIP-2 in CFs. These observations suggest that additional signaling pathways may be involved in the post-transcriptional regulations of these chemokines.

In conclusion, our study presents novel evidence for a pathogenic role of IL-21 in MIRI, most likely by promoting cardiac neutrophil infiltration and chemokine expression. A proposed scheme of the effects of IL-21 on MIRI is provided in Figure 8. Thus, IL-21 could be a promising molecular target for ameliorating reperfusion injury.

Acknowledgements

This work was supported by grants from the National Natural Science Foundation of China [No. 91639301, 81561130161, 81525003 to X.C.; No. 81400364 to N.X.; No. 81200177，81670361 to T.T.T.; No. 81600262 to X.Z.; No. 81500186 to S.F.N.], the Fundamental Research Funds for the Central Universities [2016YXMS246 to N.X.] and the Royal Society Newton Advanced Fellowship (NA140277 to Z.M.).

Author contributions

K.-J.W., S.W., J.J., T.T. and N.X. designed the experiments; K.-J.W., S.W., J.J., X.Z., M.Z., B.-J.L., Y.-Z.L. and X.-D.Z., J.-Y.L. and S.-F.N. conducted the experiments and performed data analysis; Y.-H.L., Q.W., X.T., Z.M., N.X. and X.C. reviewed and made important suggestions to the manuscript; N.X. and X.C. developed the concept and provided guidance during the study.

Conflict of interest

The authors declare no conflicts of interest.

References

Bohl S, Medway DJ, Schulz-Menger J, Schneider JE, Neubauer S, Lygate CA (2009). Refined approach for quantification of in vivo ischemia-reperfusion injury in the mouse heart. Am J Physiol Heart Circ Physiol 297: H2054-H2058.

Brenne AT, Ro TB, Waage A, Sundan A, Borset M, Hjorth-Hansen H (2002). Interleukin-21 is a growth and survival factor for human myeloma cells. Blood 99: 3756-3762.

Caruso R, Botti E, Sarra M, Esposito M, Stolfi C, Diluvio L, et al. (2009). Involvement of interleukin-21 in the epidermal hyperplasia of psoriasis. Nat Med 15: 1013-1015.

Caruso R, Fina D, Peluso I, Fantini MC, Tosti C, Del VBG, et al. (2007a). IL-21 is highly produced in Helicobacter pylori-infected gastric mucosa and promotes gelatinases synthesis. J Immunol 178: 5957-5965.

Caruso R, Fina D, Peluso I, Stolfi C, Fantini MC, Gioia V, et al. (2007b). A functional role for interleukin-21 in promoting the synthesis of the T-cell chemoattractant, MIP-3alpha, by gut epithelial cells. Gastroenterology 132: 166-175.

Clarkson BD, Ling C, Shi Y, Harris MG, Rayasam A, Sun D, et al. (2014). T cell-derived interleukin (IL)-21 promotes brain injury following stroke in mice. J Exp Med 211: 595-604.

Coquet JM, Kyparissoudis K, Pellicci DG, Besra G, Berzins SP, Smyth MJ, et al. (2007). IL-21 is produced by NKT cells and modulates NKT cell activation and cytokine production. Journal Of Immunology 178(5).

Curtis MJ, Bond RA, Spina D, Ahluwalia A, Alexander SP, Giembycz MA, et al. (2015). Experimental design and analysis and their reporting: new guidance for publication in BJP. Br J Pharmacol 172: 3461-3471.

de Totero D, Meazza R, Capaia M, Fabbi M, Azzarone B, Balleari E, et al. (2008). The opposite effects of IL-15 and IL-21 on CLL B cells correlate with differential activation of the JAK/STAT and ERK1/2 pathways. Blood 111: 517-524.

Di Fusco D, Izzo R, Figliuzzi MM, Pallone F, Monteleone G (2014). IL-21 as a therapeutic target in inflammatory disorders. Expert Opin Ther Targets 18: 1329-1338.

Ding R, Gao W, He Z, Liao M, Wu F, Zou S, et al. (2014). Effect of serum interleukin 21 on the development of coronary artery disease. APMIS 122: 842-847.

Distler JH, Jungel A, Kowal-Bielecka O, Michel BA, Gay RE, Sprott H, et al. (2005). Expression of interleukin-21 receptor in epidermis from patients with systemic sclerosis. Arthritis Rheum 52: 856-864.

Dreyer WJ, Michael LH, West MS, Smith CW, Rothlein R, Rossen RD, et al. (1991). Neutrophil accumulation in ischemic canine myocardium. Insights into time course, distribution, and mechanism of localization during early reperfusion. Circulation 84: 400-411.

Feng M, Li G, Qian X, Fan Y, Huang X, Zhang F, et al. (2012). IL-17A-producing NK cells were implicated in liver injury induced by ischemia and reperfusion. Int Immunopharmacol 13: 135-140.

Frangogiannis NG, Entman ML (2005). Chemokines in myocardial ischemia. Trends Cardiovasc Med 15: 163-169.

Gharibi T, Majidi J, Kazemi T, Dehghanzadeh R, Motallebnezhad M, Babaloo Z (2016). Biological effects of IL-21 on different immune cells and its role in autoimmune diseases. Immunobiology 221: 357-367.

Hofmann U, Frantz S (2015). Role of lymphocytes in myocardial injury, healing, and remodeling after myocardial infarction. Circ Res 116: 354-367.

Jungel A, Distler JH, Kurowska-Stolarska M, Seemayer CA, Seibl R, Forster A, et al. (2004). Expression of interleukin-21 receptor, but not interleukin-21, in synovial fibroblasts and synovial macrophages of patients with rheumatoid arthritis. Arthritis Rheum 50: 1468-1476.

Kilkenny C, Browne W, Cuthill IC, Emerson M, Altman DG (2010). Animal research: reporting in vivo experiments: the ARRIVE guidelines. Br J Pharmacol 160: 1577-1579.

Lafontant PJ, Burns AR, Donnachie E, Haudek SB, Smith CW, Entman ML (2006). Oncostatin M differentially regulates CXC chemokines in mouse cardiac fibroblasts. Am J Physiol Cell Physiol 291: C18-C26.

Lee AS, Wang GJ, Chan HC, Chen FY, Chang CM, Yang CY, et al. (2012). Electronegative low-density lipoprotein induces cardiomyocyte apoptosis indirectly through endothelial cell-released chemokines. Apoptosis 17: 1009-1018.

Li X, Liu Y, Wang L, Li Z, Ma X (2015). Unfractionated heparin attenuates LPS-induced IL-8 secretion via PI3K/Akt/NF-kappaB signaling pathway in human endothelial cells. Immunobiology 220: 399-405.

Li X, Tupper JC, Bannerman DD, Winn RK, Rhodes CJ, Harlan JM (2003). Phosphoinositide 3 kinase mediates Toll-like receptor 4-induced activation of NF-kappa B in endothelial cells. Infect Immun 71: 4414-4420.

Li Y, Garson CD, Xu Y, Beyers RJ, Epstein FH, French BA, et al. (2007). Quantification and MRI validation of regional contractile dysfunction in mice post myocardial infarction using high resolution ultrasound. Ultrasound Med Biol 33: 894-904.

Liao YH, Xia N, Zhou SF, Tang TT, Yan XX, Lv BJ, et al. (2012). Interleukin-17A contributes to myocardial ischemia/reperfusion injury by regulating cardiomyocyte apoptosis and neutrophil infiltration. J Am Coll Cardiol 59: 420-429.

Lin CH, Cheng HW, Ma HP, Wu CH, Hong CY, Chen BC (2011). Thrombin induces NF-kappaB activation and IL-8/CXCL8 expression in lung epithelial cells by a Rac1-dependent PI3K/Akt pathway. J Biol Chem 286: 10483-10494.

Lopez-Neblina F, Toledo-Pereyra LH (2006). Phosphoregulation of signal transduction pathways in ischemia and reperfusion. J Surg Res 134: 292-299.

Lowell CA, Fumagalli L, Berton G (1996). Deficiency of Src family kinases p59/61hck and p58c-fgr results in defective adhesion-dependent neutrophil functions. J Cell Biol 133: 895-910.

McGrath JC, Lilley E (2015). Implementing guidelines on reporting research using animals (ARRIVE etc.): new requirements for publication in BJP. Br J Pharmacol 172: 3189-3193.

Metzler B, Mair J, Lercher A, Schaber C, Hintringer F, Pachinger O, et al. (2001). Mouse model of myocardial remodelling after ischemia: role of intercellular adhesion molecule-1. Cardiovasc Res 49: 399-407.

Michael LH, Entman ML, Hartley CJ, Youker KA, Zhu J, Hall SR, et al. (1995). Myocardial ischemia and reperfusion: a murine model. Am J Physiol 269: H2147-H2154.

Monteleone G, Caruso R, Fina D, Peluso I, Gioia V, Stolfi C, et al. (2006). Control of matrix metalloproteinase production in human intestinal fibroblasts by interleukin 21. Gut 55: 1774-1780.

Monteleone G, Pallone F, Macdonald TT (2009). Interleukin-21 (IL-21)-mediated pathways in T cell-mediated disease. Cytokine Growth Factor Rev 20: 185-191.

Parrish-Novak J, Dillon SR, Nelson A, Hammond A, Sprecher C, Gross JA, et al. (2000). Interleukin 21 and its receptor are involved in NK cell expansion and regulation of lymphocyte function. Nature 408: 57-63.

Pelletier M, Bouchard A, Girard D (2004). In vivo and in vitro roles of IL-21 in inflammation. J Immunol 173: 7521-7530.

Puga I, Cols M, Barra CM, He B, Cassis L, Gentile M, et al. (2012) B cell-helper neutrophils stimulate the diversification andproduction of immunoglobulin in the marginal zone of the spleen. Nat.Immunol 13(2): 170-180.

Ruddy MJ, Shen F, Smith JB, Sharma A, Gaffen SL (2004). Interleukin-17 regulates expression of the CXC chemokine LIX/CXCL5 in osteoblasts: implications for inflammation and neutrophil recruitment. J Leukoc Biol 76: 135-144.

Rui T, Cepinskas G, Feng Q, Ho YS, Kvietys PR (2001). Cardiac myocytes exposed to anoxia-reoxygenation promote neutrophil transendothelial migration. Am J Physiol Heart Circ Physiol 281: H440-H447.

Siemsen DW, Schepetkin IA, Kirpotina LN, Lei B, Quinn MT (2007). Neutrophil isolation from

nonhuman species. Methods Mol Biol 412: 21-34.

Spolski R, Leonard WJ (2014). Interleukin-21: a double-edged sword with therapeutic potential. Nat Rev Drug Discov 13: 379-395.

Spolski R, Leonard WJ (2008). Interleukin-21: basic biology and implications for cancer and autoimmunity. Annu Rev Immunol 26: 57-79.

Spolski R, Wang L, Wan CK, Bonville CA, Domachowske JB, Kim HP, et al. (2012). IL-21 promotes the pathologic immune response to pneumovirus infection. J Immunol 188: 1924-1932.

Stephanou A (2002). Activated STAT-1 pathway in the myocardium as a novel therapeutic target in ischaemia/reperfusion injury. Eur Cytokine Netw 13: 401-403.

Sutton CE, Lalor SJ, Sweeney CM, Brereton CF, Lavelle EC, Mills KH (2009). Interleukin-1 and IL-23 induce innate IL-17 production from gammadelta T cells, amplifying Th17 responses and autoimmunity. Immunity 31: 331-341.

Takeda Y, Nara H, Araki A, Asao H (2014). Human peripheral neutrophils express functional IL-21 receptors. Inflammation 37: 1521-1532.

Tarnavski O, McMullen JR, Schinke M, Nie Q, Kong S, Izumo S (2004). Mouse cardiac surgery: comprehensive techniques for the generation of mouse models of human diseases and their application for genomic studies. Physiol Genomics 16: 349-360.

Timmers L, Pasterkamp G, de Hoog VC, Arslan F, Appelman Y, de Kleijn DP (2012). The innate immune response in reperfused myocardium. Cardiovasc Res 94: 276-283.

Turer AT, Hill JA (2010). Pathogenesis of myocardial ischemia-reperfusion injury and rationale for therapy. Am J Cardiol 106: 360-368.

Turner NA, Das A, O'Regan DJ, Ball SG, Porter KE (2011). Human cardiac fibroblasts express ICAM-1, E-selectin and CXC chemokines in response to proinflammatory cytokine stimulation. Int J Biochem Cell Biol 43: 1450-1458.

Tzartos JS, Craner MJ, Friese MA, Jakobsen KB, Newcombe J, Esiri MM, et al. (2011). IL-21 and IL-21 receptor expression in lymphocytes and neurons in multiple sclerosis brain. Am J Pathol 178: 794-802.

Van der Heiden K, Cuhlmann S, Luong LA, Zakkar M, Evans PC (2010). Role of nuclear factor kappaB in cardiovascular health and disease. Clin Sci (Lond) 118: 593-605.
Vinten-Johansen J (2004). Involvement of neutrophils in the pathogenesis of lethal myocardial reperfusion injury. Cardiovasc Res 61: 481-497.

Wang T, Cunningham A, Dokun AO, Hazarika S, Houston K, Chen L, et al. (2015). Loss of interleukin-21 receptor activation in hypoxic endothelial cells impairs perfusion recovery after hindlimb ischemia. Arterioscler Thromb Vasc Biol 35: 1218-1225.

Weir RA, Miller AM, Petrie CJ, Clements S, Steedman T, Dargie HJ, et al. (2012). Interleukin-21--a biomarker of importance in predicting myocardial function following acute infarction? Cytokine 60: 220-225.

Xing R, Jin Y, Sun L, Yang L, Li C, Li Z, et al. (2016). Interleukin-21 Induces Migration and Invasion of Fibroblast-like Synoviocytes from Patients with Rheumatoid Arthritis. Clin Exp Immunol 184:147-58.

Yan X, Anzai A, Katsumata Y, Matsuhashi T, Ito K, Endo J, et al. (2013). Temporal dynamics of cardiac immune cell accumulation following acute myocardial infarction. J Mol Cell Cardiol 62: 24-35.

Figure legends

Figure 1. IL-21 and IL-21R are elevated during the acute phase of myocardial ischemia/reperfusion injury (MIRI) and $CD4^+$T cells are the major source of IL-21 in the ischemic myocardium. The time course of changes in the (A) mRNA and (B) protein expression of IL-21 in the myocardium following MIRI were measured by quantitative real-time PCR and western blotting, respectively (n=6 per group). The time course of changes in the (C) mRNA and (D) protein expression of IL-21R in the myocardium following MIRI were measured via quantitative real-time PCR and western blotting, respectively (n=6 per group). (E) The infiltrated $IL\text{-}21^+$ leukocytes in myocardial I/R mice after 6 hours of reperfusion were analyzed by flow cytometry. $CD45^+$ cells were isolated and restimulated. The $IL\text{-}21^+$ $CD45^+$ cells were further analyzed for CD3, CD4 and γδTCR expression to detect the cellular source of IL-21. The proportion of different IL-21-secreting cells in the $IL\text{-}21^+CD45^+$ cells were quantitatively analyzed (n=5 per group). *P <0.05 versus sham.

Figure 2. IL-21 neutralization attenuates, whereas exogenous IL-21 aggravates, myocardial injury. **(A)** Representative images of left ventricular slices from different groups 1 day after reperfusion. The non-ischemic area is indicated in blue, the area at risk (AAR) in red, and the infarct area (I) in white. **(B)** Quantification of infarct size of myocardial tissues 1 day after reperfusion. **(C)** Serum cTnT was measured 1 day after reperfusion. **(D)** Representative M-mode echocardiographic images of the left ventricular 1 day after reperfusion. **(E)** Left ventricular ejection fraction (EF) and fractional shortening (FS) were measured via echocardiography 1 day after reperfusion. *$P < 0.05$ versus isotype; #$P < 0.05$ versus vehicle. Isotype, n=9; anti-IL-21, n=9; vehicle, n=11; IL-21, n=10.

Figure 3. IL-21 increases the number of cardiac-infiltrating neutrophils and myocardial expression of keratinocyte-derived chemokine (KC) and macrophage inflammatory protein-2 (MIP-2) following myocardial ischemia/reperfusion injury (MIRI), while anti-IL-21 mAb reduced cardiac-infiltrating neutrophils and the expression of KC and MIP-2. (A-D) The number, percentage and representative contour plots of $CD11b^+Gr\text{-}1^+$ neutrophils infiltrating the myocardium after 30 minutes of ischemia and 3 hours of reperfusion were analyzed via flow cytometry (n=5 per group). (E-F) The mRNA expression of KC, MIP-2, and LIX in the

myocardium after 30 minutes of ischemia followed by 30 minutes or 3 hours of reperfusion was analyzed via real-time PCR (n=5 per group). *P < 0.05 versus Sham; #P < 0.05 versus vehicle or isotype.

Figure 4. IL-21 induces neutrophil migration and the expression of keratinocyte-derived chemokine (KC) and macrophage inflammatory protein-2 (MIP-2) in cardiomyocytes (CMs) and cardiac fibroblasts (CFs). **(A)** Neutrophil migration in the presence of conditioned supernatants from stimulated CMs (upper) and CFs (lower) was measured by transwell assay. The values were normalized relative to those of the medium from unstimulated CMs or CFs (control). **(B)** The mRNA expression of KC and MIP-2 in response to 1 h of stimulation with IL-21(100 $ng \cdot mL^{-1}$) in CMs (left) and CFs (right). **(C)** ELISA results of KC and MIP-2 levels in the supernatants of CMs (left) and CFs (right) stimulated by IL-21(100 $ng \cdot mL^{-1}$) for 24 h. H_2O_2 (100 μM) or TNF-α (5 $ng \cdot mL^{-1}$) served as positive controls for CMs and CFs, respectively. IL-21-alone control media was from unstimulated cells 'spiked' with IL-21. Data are representative of five independent experiments. *$P < 0.05$ versus control.

Figure 5. Activation of the ERK, p38 MAPK, Akt, NF-κB, STAT1 and STAT3 signaling pathways in the myocardium after the administration of exogenous IL-21. **(A)** Representative western blots showing the activation of different signaling pathways 10 min after reperfusion in the myocardium after IL-21 administration. **(B)** Quantitative analysis of the levels of phospho-/total-ERK, p38 MAPK, Akt, NF-κB, STAT1 and STAT3 signaling pathways 10 min after reperfusion in different groups (n=6 per group). **(C)** Representative western blots showing the activation of different signaling pathways 30 min after reperfusion in the myocardium after IL-21 administration. **(D)** Quantitative analysis of the levels of phospho-/total-ERK, p38 MAPK, Akt, NF-κB, STAT1 and STAT3 signaling pathways 30 min after reperfusion in different groups (n=6 per group). *$P < 0.05$ versus sham; #$P < 0.05$ versus vehicle.

Figure 6. Direct effects of IL-21 on the activation of Akt, p38 MAPK and NF-κB signaling in isolated cardiomyocytes (CMs) and cardiac fibroblasts (CFs). **(A-B)** Representative western blots showing the phospho-/total-Akt, p38 MAPK and NF-κB p65 levels in CMs and CFs unstimulated (control) or stimulated with IL-21 (100 $ng \cdot mL^{-1}$) for indicated durations. **(C-D)** Quantitative analysis of the phospho-/total- Akt, p38 MAPK and NF-κB p65 levels in CMs and

CFs. Data are representative of five independent experiments. *$P < 0.05$ versus control.

Figure 7. IL-21-induced chemokine expression is Akt/NF-κB or p38 MAPK/NF-κB dependent. **(A)** Cardiomyocytes (CMs) were pre-treated for 1 h with an Akt inhibitor (LY294002, 10 μM) or an NF-κB inhibitor (BAY11-7082, 10 μM), followed by IL-21 (100 ng·mL^{-1}) stimulation for 1 h. The expression of keratinocyte-derived chemokine (KC) and macrophage inflammatory protein-2 (MIP-2) was measured via real-time PCR. **(B)** CMs were pre-treated for 1 h with the indicated inhibitors, followed by IL-21 stimulation for 24 h. Concentrations of KC and MIP-2 in the culture media were measured via ELISA. **(C)** Cardiac fibroblasts (CFs) were pre-treated for 1 h with a p38 MAPK inhibitor (SB203580, 10 μM) or an NF-κB inhibitor (BAY11-7082, 10 μM), followed by IL-21 (100 ng·mL^{-1}) stimulation for 1 h. The expression of KC and MIP-2 was measured via real-time PCR. **(D)** CFs were pre-treated for 1 h with the indicated inhibitors, followed by IL-21 stimulation for 24 h. Concentrations of KC and MIP-2 in the culture media were measured via ELISA. **(E)** CMs were pre-treated with LY294002 and **(F)** CFs were pre-treated with SB203580 and then cells were stimulated with IL-21 or vehicle for 1 h. NF-κB p65 phosphorylation was analyzed via western blotting. Representative western blot images (left) and quantitative analyses (right) are shown. Data are representative of five independent experiments. *$P < 0.05$ versus control; #$P < 0.05$ versus IL-21.

Figure 8. Schematic illustration of the IL-21-mediated effects on neutrophil recruitment in myocardial ischemia/reperfusion injury (MIRI). MIRI induces the up-regulation of IL-21 in the myocardium, which directly acts on cardiomyocytes (CMs) and cardiac fibroblasts (CFs) to promote the mRNA expression and production of keratinocyte-derived chemokine (KC) and macrophage inflammatory protein-2 (MIP-2) via the activation of Akt/NF-κB or p38 MAPK/NF-κB signaling in CMs or CFs, respectively. KC and MIP-2 are potent neutrophil chemoattractants, which recruit neutrophils into the injured myocardium.

Figure 1

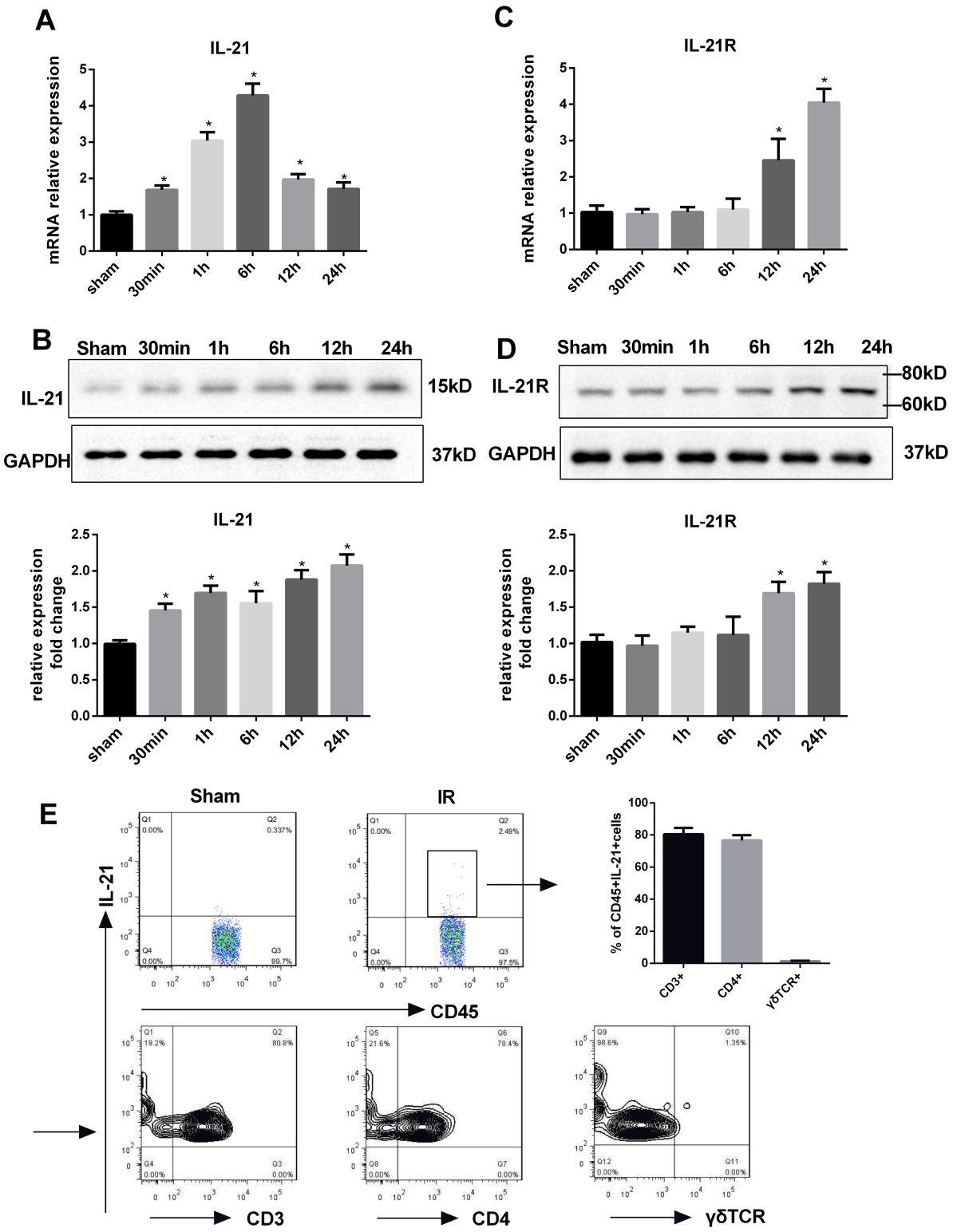
A
IL-21
mRNA relative expression
sham
30min
1h
6h
12h
24h
C
IL-21R
mRNA relative expression
B
Sham 30min 1h 6h 12h 24h
IL-21
15kD
GAPDH
37kD
D
Sham 30min 1h 6h 12h 24h
IL-21R
80kD
60kD
GAPDH
37kD
IL-21
relative expression fold change
IL-21R
relative expression fold change
E
Sham
IR
IL-21
CD45
CD3
CD4
γδTCR
% of CD45+IL-21+cells
CD3+
CD4+
γδTCR+

Figure 2

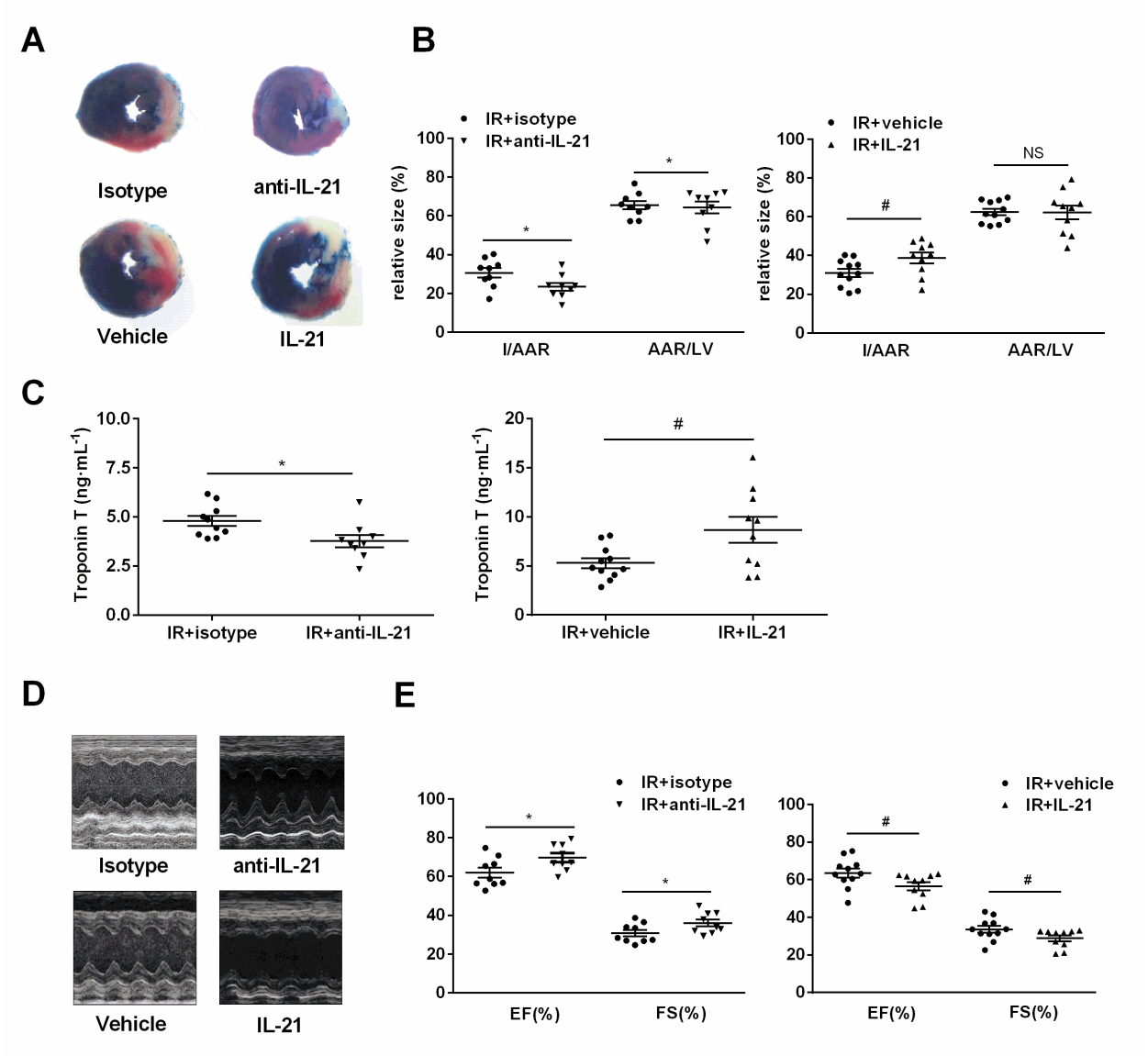
A
Isotype
anti-IL-21
Vehicle
IL-21
B
IR+isotype
IR+anti-IL-21
relative size (%)
I/AAR
AAR/LV
IR+vehicle
IR+IL-21
NS
C
Troponin T (ng·mL-1)
IR+isotype
IR+anti-IL-21
IR+vehicle
IR+IL-21
D
Isotype
anti-IL-21
Vehicle
IL-21
E
IR+isotype
IR+anti-IL-21
EF(%)
FS(%)
IR+vehicle
IR+IL-21

Figure 3

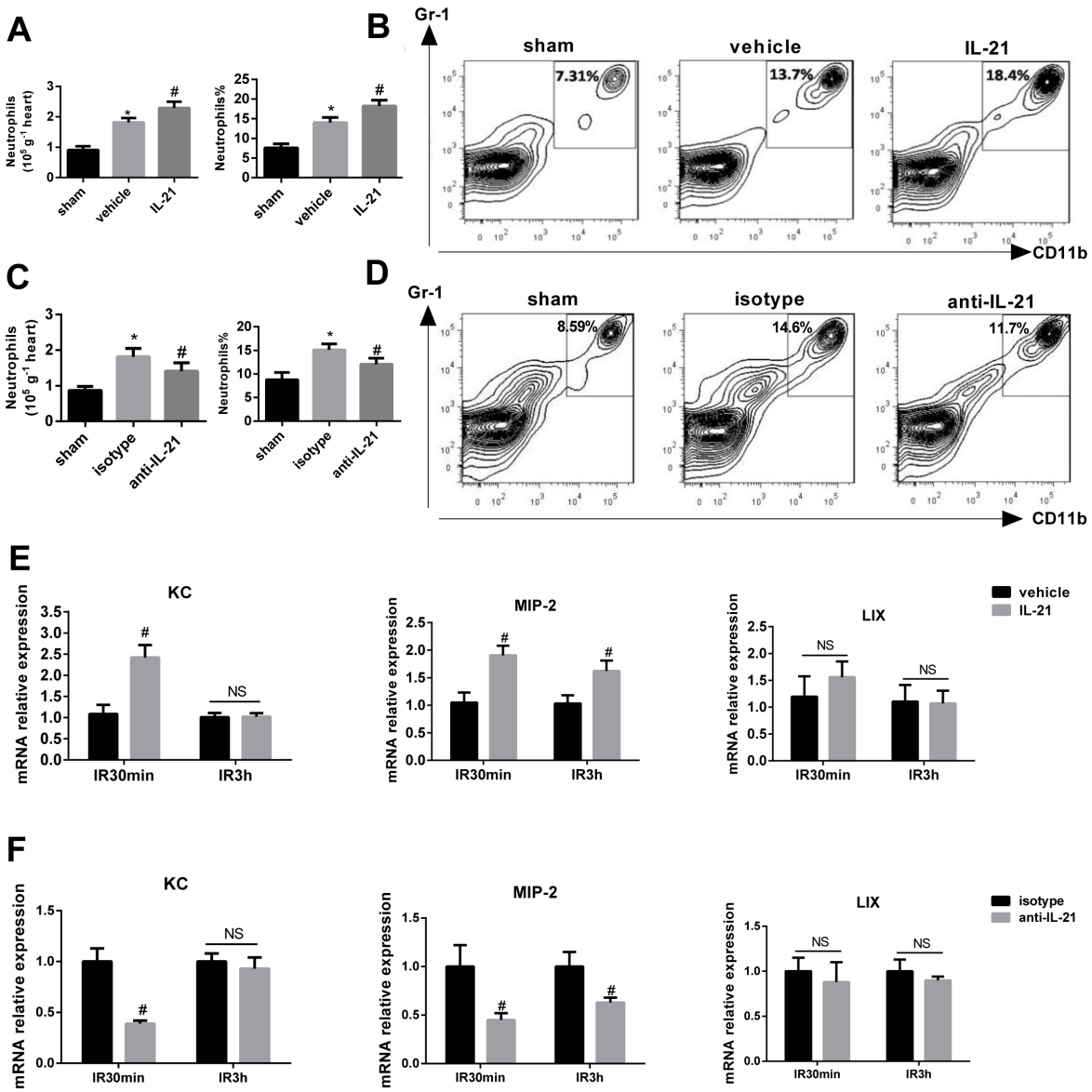
A
Neutrophils (10^5 g^{-1} heart)
Neutrophils%
sham
vehicle
IL-21
B
Gr-1
CD11b
sham
vehicle
IL-21
7.31%
13.7%
18.4%
C
Neutrophils (10^5 g^{-1} heart)
Neutrophils%
sham
isotype
anti-IL-21
D
Gr-1
CD11b
sham
isotype
anti-IL-21
8.59%
14.6%
11.7%
E
KC
MIP-2
LIX
mRNA relative expression
IR30min
IR3h
NS
vehicle
IL-21
F
KC
MIP-2
LIX
mRNA relative expression
IR30min
IR3h
NS
isotype
anti-IL-21

Figure 4

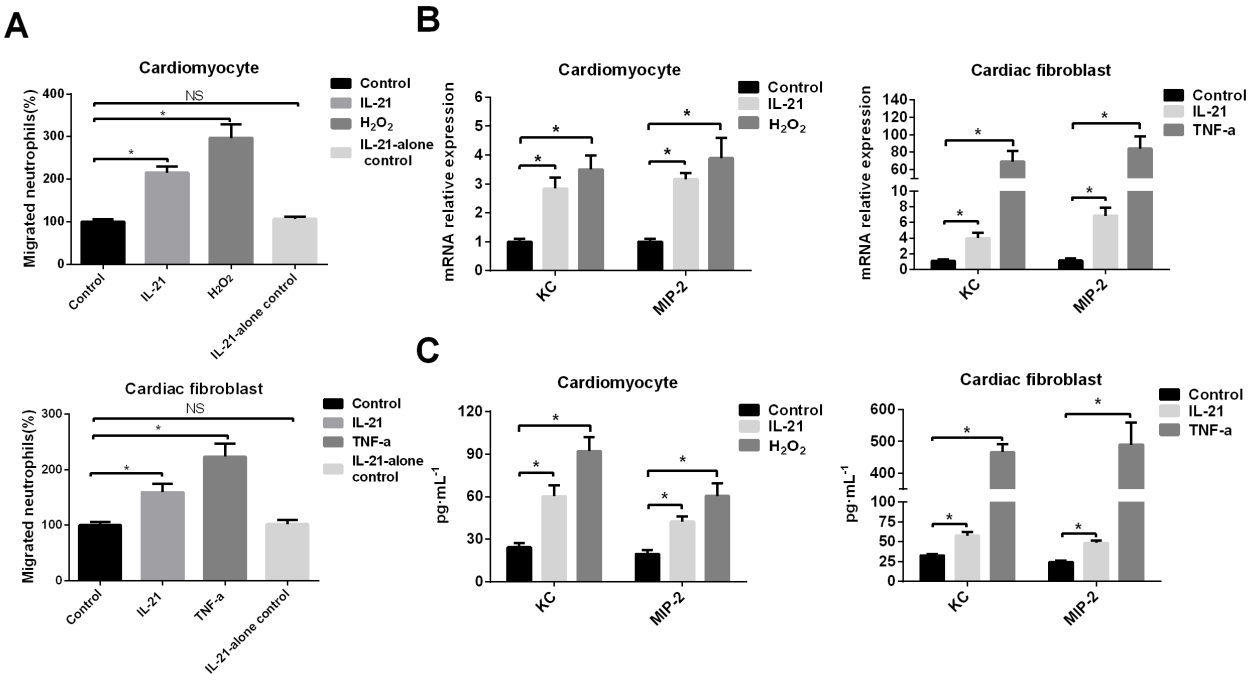
A
Cardiomyocyte
Migrated neutrophils(%)
NS
Control
IL-21
H2O2
IL-21-alone control
B
Cardiomyocyte
mRNA relative expression
KC
MIP-2
Control
IL-21
H2O2
Cardiac fibroblast
TNF-a
C
pg·mL-1

Figure 5

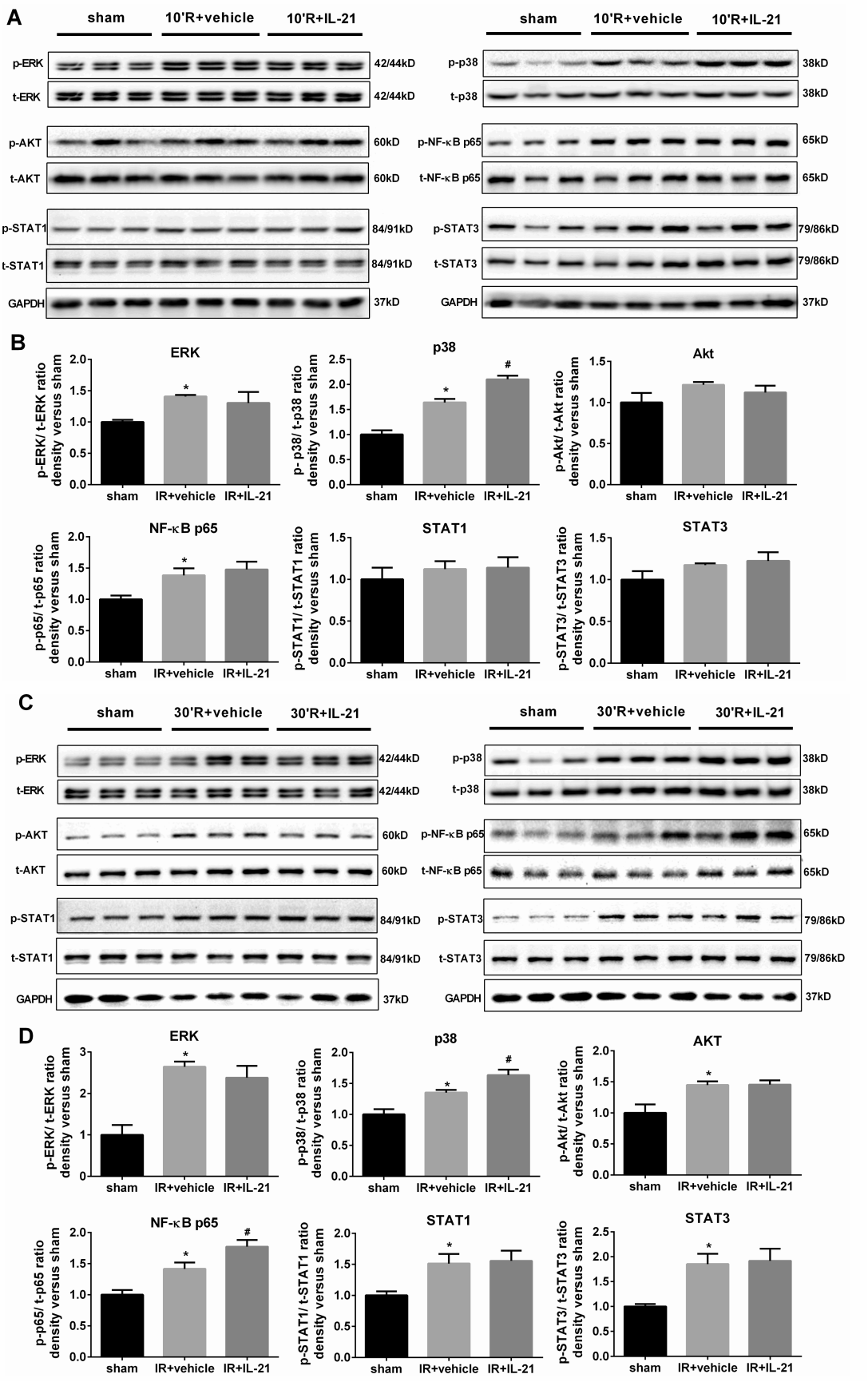
A
sham
10'R+vehicle
10'R+IL-21
p-ERK
t-ERK
p-AKT
t-AKT
p-STAT1
t-STAT1
GAPDH
42/44kD
60kD
84/91kD
37kD
p-p38
t-p38
p-NF-κB p65
t-NF-κB p65
p-STAT3
t-STAT3
38kD
65kD
79/86kD
B
ERK
p38
Akt
NF-κB p65
STAT1
STAT3
p-ERK/ t-ERK ratio density versus sham
p- p38/ t-p38 ratio density versus sham
p-Akt/ t-Akt ratio density versus sham
p-p65/ t-p65 ratio density versus sham
p-STAT1/ t-STAT1 ratio density versus sham
p-STAT3/ t-STAT3 ratio density versus sham
sham
IR+vehicle
IR+IL-21
C
30'R+vehicle
30'R+IL-21
D
AKT

Figure 6

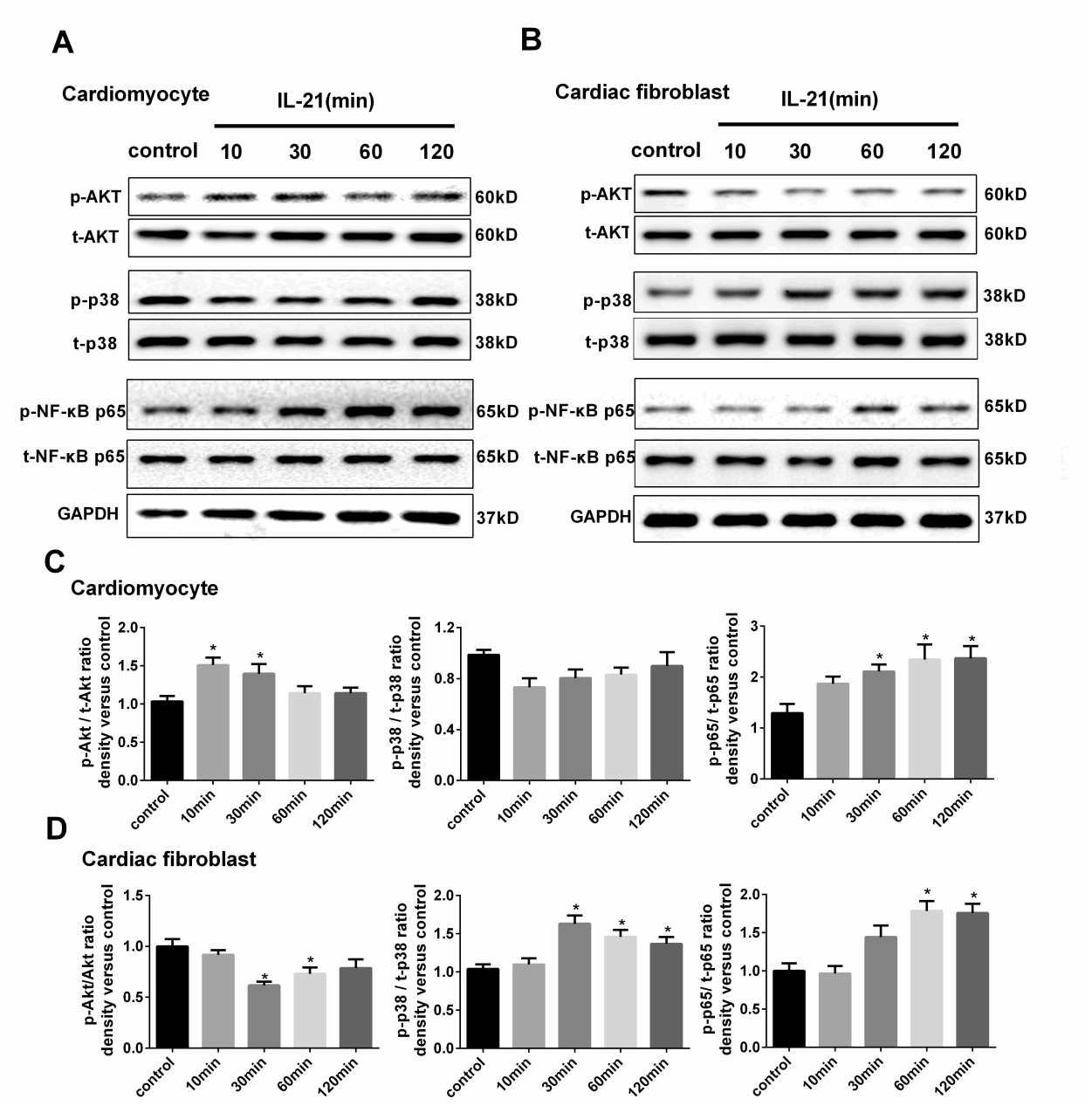
A
Cardiomyocyte
IL-21(min)
control
10
30
60
120
p-AKT
t-AKT
p-p38
t-p38
p-NF-κB p65
t-NF-κB p65
GAPDH
60kD
60kD
38kD
38kD
65kD
65kD
37kD
B
Cardiac fibroblast
IL-21(min)
control
10
30
60
120
p-AKT
t-AKT
p-p38
t-p38
p-NF-κB p65
t-NF-κB p65
GAPDH
60kD
60kD
38kD
38kD
65kD
65kD
37kD
C
Cardiomyocyte
p-Akt / t-Akt ratio density versus control
p-p38 / t-p38 ratio density versus control
p-p65/ t-p65 ratio density versus control
control
10min
30min
60min
120min
D
Cardiac fibroblast
p-Akt/Akt ratio density versus control
p-p38 / t-p38 ratio density versus control
p-p65/ t-p65 ratio density versus control
control
10min
30min
60min
120min

Figure 7

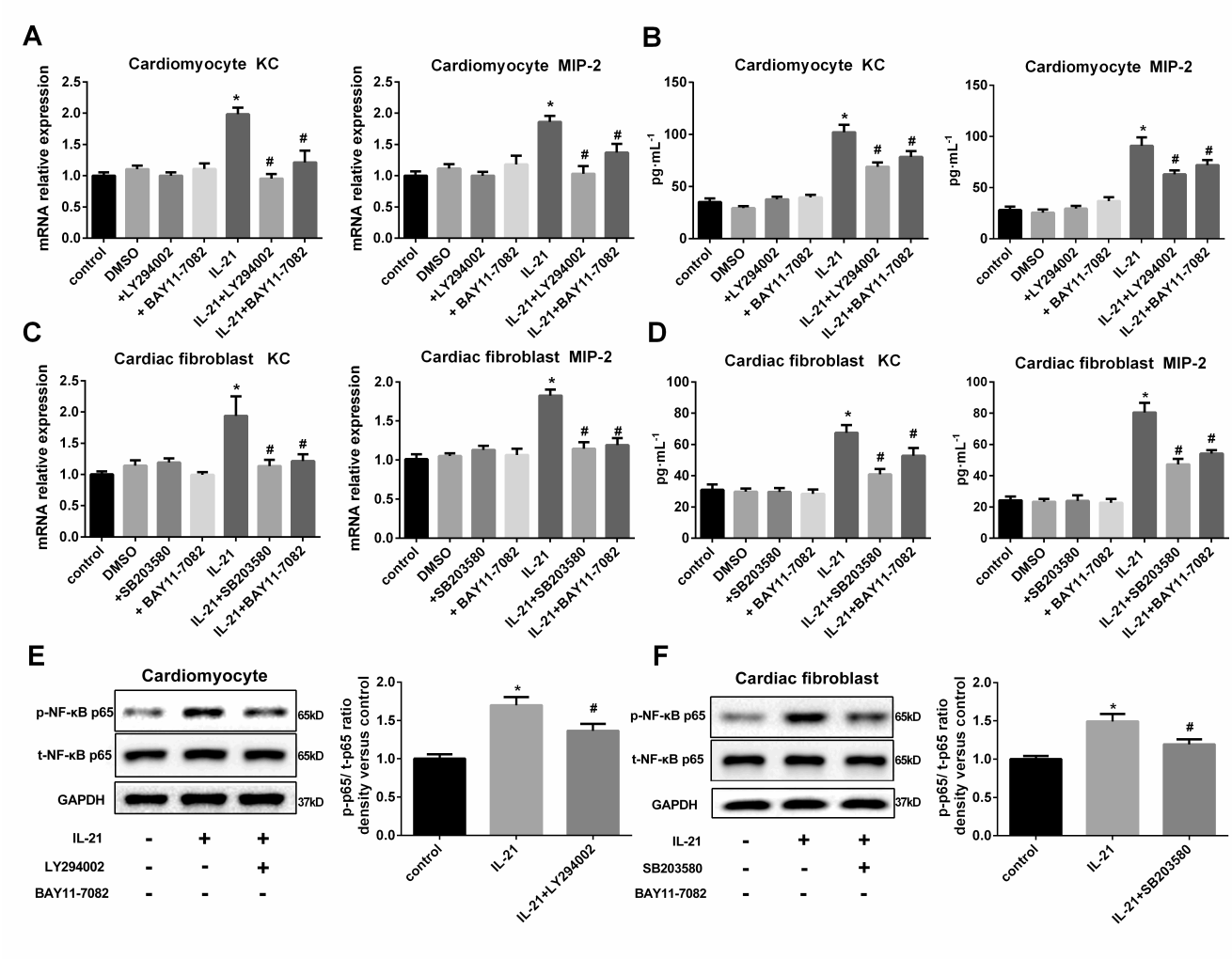
A
Cardiomyocyte KC
mRNA relative expression
Cardiomyocyte MIP-2
mRNA relative expression
B
Cardiomyocyte KC
pg·mL-1
Cardiomyocyte MIP-2
pg·mL-1
control
DMSO
+LY294002
+ BAY11-7082
IL-21
IL-21+LY294002
IL-21+BAY11-7082
C
Cardiac fibroblast KC
mRNA relative expression
Cardiac fibroblast MIP-2
mRNA relative expression
D
Cardiac fibroblast KC
pg·mL-1
Cardiac fibroblast MIP-2
pg·mL-1
control
DMSO
+SB203580
+ BAY11-7082
IL-21
IL-21+SB203580
IL-21+BAY11-7082
E
Cardiomyocyte
p-NF-κB p65
65kD
t-NF-κB p65
65kD
GAPDH
37kD
IL-21
LY294002
BAY11-7082
p-p65/ t-p65 ratio
density versus control
control
IL-21
IL-21+LY294002
F
Cardiac fibroblast
p-NF-κB p65
65kD
t-NF-κB p65
65kD
GAPDH
37kD
IL-21
SB203580
BAY11-7082
p-p65/ t-p65 ratio
density versus control
control
IL-21
IL-21+SB203580

Figure 8

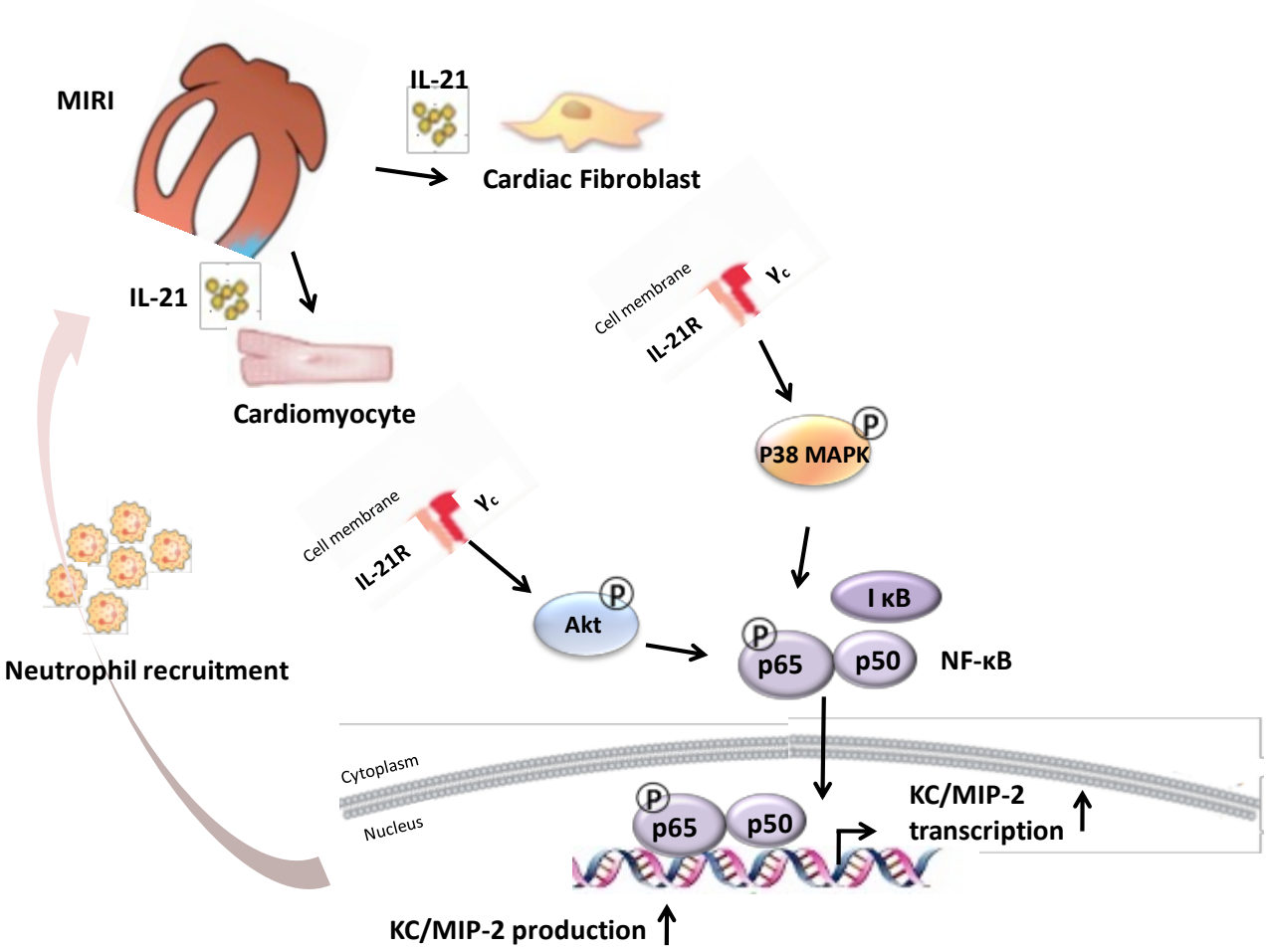
MIRI
IL-21
Cardiac Fibroblast
IL-21
Cardiomyocyte
Cell membrane
IL-21R
γc
P38 MAPK
P
Cell membrane
IL-21R
γc
Akt
P
I κB
P
p65
p50
NF-κB
Neutrophil recruitment
Cytoplasm
Nucleus
P
p65
p50
KC/MIP-2
transcription
KC/MIP-2 production

SUPPLEMENTARY INFORMATION

TITLE: IL-21 promotes myocardial ischemia/reperfusion injury through modulation of neutrophil infiltration

AUTHORS: Kejing Wang[1,2]†, Shuang Wen[1,2]†, Jiao Jiao[1,2]†, Tingting Tang[1,2], Xin Zhao[3], Min Zhang[1,2], Bingjie Lv[1,2], Yuzhi Lu[1,2], Xingdi Zhou[1,2], Jingyong Li[1,2], Shaofang Nie[1,2], Yuhua Liao[1,2], Qing Wang[4], Xin Tu[4], Ziad Mallat[5], Ni Xia[1,2]*, Xiang Cheng[1,2]*

Supplemental Table1 Primer sequences in qRT-PCR

Gene	*Forward (5'-3')*	*Reverse (5'-3')*
IL-21	GGACCCTTGTCTGTCTGGTAG	TGTGGAGCTGATAGAAGTTCAGG
IL-21R	TGTCTCAATTCCTGTCCGATGA	GCACGTAGTTGGAGGGTTCG
KC	GCTGGGATTCACCTCAAGAA	CTTGGGGACACCTTTTAGCA
MIP2	CGCCCAGACAGAAGTCATAG	TCCTCCTTTCCAGGTCAGTTA
LIX	GGTCCACAGTGCCCTACG	GCGAGTGCATTCCGCTTA
β-actin	AAGGCCAACCGTGAAAAGAT	GTGGTACGACCAGAGGCATAC

Figure S1

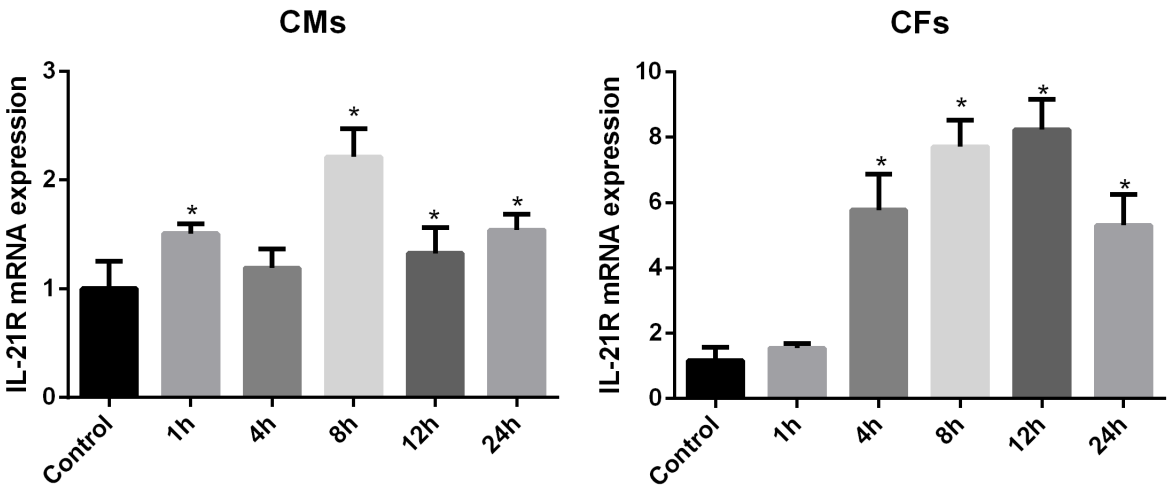

Figure S1 H_2O_2 induces IL-21R gene expression in CMs and TNF-α induces IL-21R gene expression in CFs. Serum-starved CMs were treated with H_2O_2 (100 μM) and CFs were treated with TNF-α (5 ng·mL^{-1}) for different periods of time. The time course of changes in the mRNA expression of IL-21R was measured via quantitative real-time PCR. Data are shown as the means ± SEM of five individual experiments. * $P < 0.05$ versus control.

Figure S2

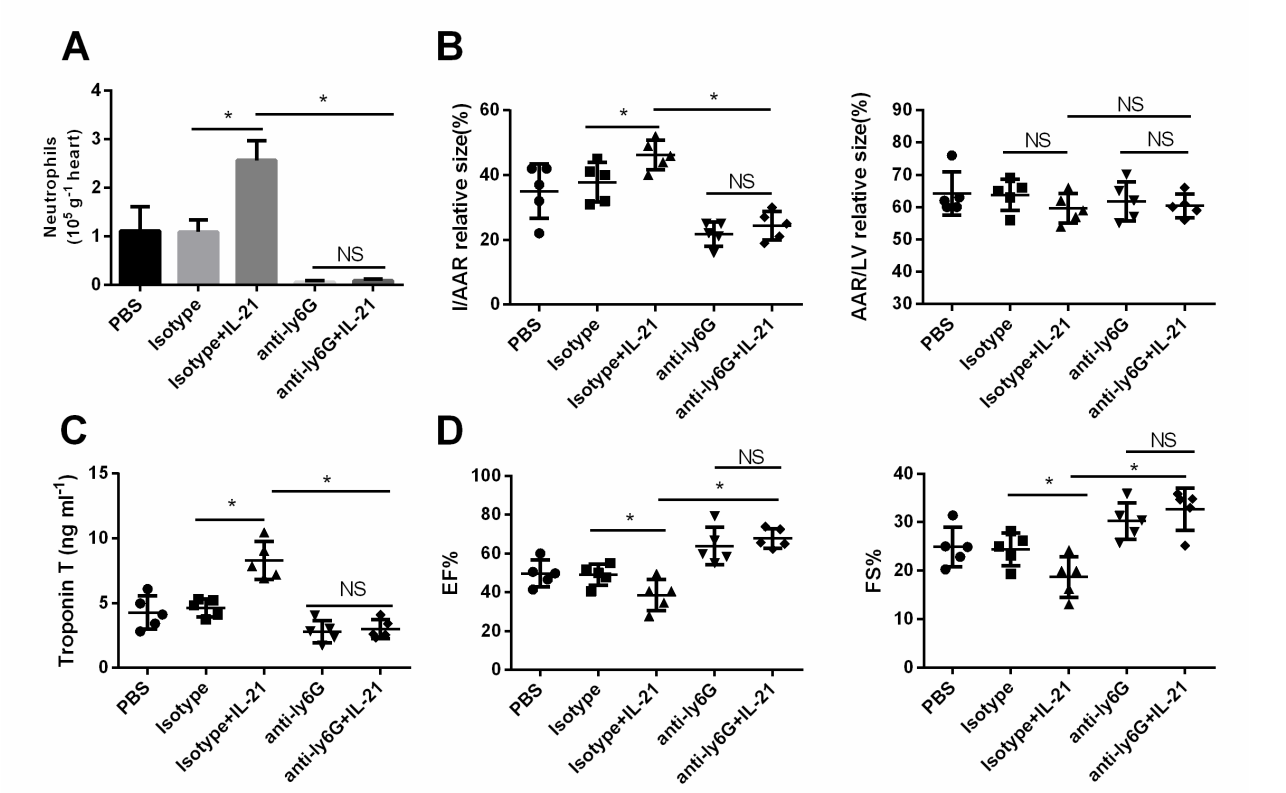

Figure S2 Depletion of neutrophils ameliorated the IL-21-induced myocardial ischemic injury. (A) The number of $CD11b^{+}Gr\text{-}1^{+}$ neutrophils infiltrating the myocardium after 30 minutes of ischemia and 3 hours of reperfusion was analyzed via flow cytometry. (B) Quantification of infarct size of myocardial tissues 1 day after reperfusion. (C) Serum cTnT was measured 1 day after reperfusion. (D) Left ventricular ejection fraction (EF) and fractional shortening (FS) were measured via echocardiography 1 day after reperfusion (n=5 per group). * $P < 0.05$ versus the other group.

Figure S3

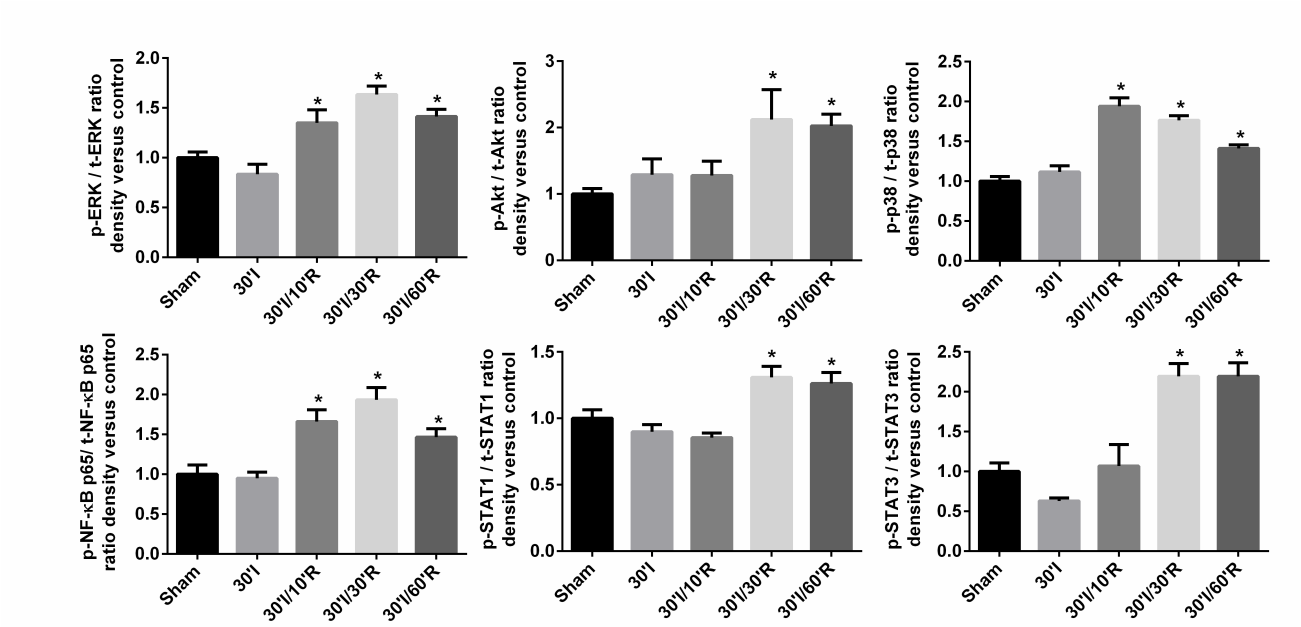

Figure S3 Temporal changes of different signaling pathways in the ischemic myocardium at different time points after reperfusion. Quantitative analysis of the phospho-/total-ERK, Akt, p38 MAPK, NF-κB p65, STAT1 and STAT3 levels in the myocardium at the indicated time points are shown (n=6 per group). * $P < 0.05$ versus control.